Interaction Notes

Note 619

30 September 2010

Pulsed Excitations of Resonators

Jürgen Nitsch*, Sergey Tkachenko*, and Stefan Potthast**

*Otto-von-Guericke University Magdeburg
Department of Electrical Engineering and Information Technology

**Federal Armed Forces Research Institute for Protection Technologies

Abstract

In this paper, electromagnetic quantities (such as currents and voltages on irradiated transmission lines and electromagnetic fields) are described in time domain, as they typically occur in resonant systems. Electric oscillating circuits, transmission lines, and cavity resonators are considered resonators. It turns out that for realistic high-frequency pulsed excitations all systems show transients with amplitudes that greatly exceed those of the steady state. Furthermore, pronounced beat effects can be seen, which may have implications especially in the interaction with non-linear electronic components (demodulation). Experiments show that those transients can disrupt or even destroy digital electronics. This is a phenomenon that is often ignored in conventional EMC testing.

This work was sponsored by the German Federal Armed Forces Research Institute for Protection Technologies (WIS), Munster.

1 Introduction

Modern engineering systems are increasingly using intelligent information technology components with high packing density and, likewise, increasing sensitivity to electromagnetic interference. Similarly, the threat of such systems to excitation is growing with the increasing number of strong HPEM sources (HPM, UWB, DS). Excitations of systems are almost always enhanced by the systems themselves, or by their components due to resonance phenomena. Resonators or Mode Stirred Chambers (MSC) that show these resonance phenomena are formed, in principle, by any enclosure, especially if their walls are made of metal. Thus nearly every real system is affected, such as cabins of vehicles, aircraft, containers or other shielding enclosures.

Even if relevant standards include these resonance phenomena, they still only take into account the steady state. Any response of a resonator that is excited by an impulse (even turning a CW excitation on and off) contains the steady state part as well as a transient part. Although less attention is paid to this transient part in the standardization, it can experimentally be shown that it is accountable for damage mechanisms [1]. Therefore, for future hardening measures these transient effects on digital electronics should be taken into consideration and be included in corresponding standards. If resonators (e.g. circuits, multiports, lines, MSCs) are excited by pulsed generators, one has to expect a strong transient response for an appropriate choice of pulse parameters: rise time, duration, maximal amplitude, carrier frequency, repetition rate, etc. This hypothesis will be proven in this paper by investigating different configurations of resonators.

Resonators can be described either by an oscillating equation (restricted here to a second order ODE) or a wave equation. The solution of these equations can be represented in closed form by the matrizant (product integral) [2]. Also for a three dimensional resonator (MSC, shielding box, etc.) the single mode functions fulfill an oscillating equation at any point inside the resonator. The matrizant (Green's function) can also be interpreted as a transfer function. Different pulsed sources are used for the general solution.

A variety of physical and technical systems that are excited by external forces can be mathematically described in terms of harmonic oscillator models. In general, the relevant equations describing these coupled oscillators contain non – linearities. The investigation of such systems is very complicated and will be performed with the aid of ordinary differential equations. This work will, however, be restricted to linear systems, mainly in time domain. The effects appear when the external exciting forces are switched on – and/or off, which in reality is always the case.

The paper is organized as follows: Section 2 starts with a single oscillator model as a basic element for the following considerations. The oscillator is excited by different signals: a turned on sinusoidal signal, a turned off sinusoidal signal, a double exponential signal, etc. The calculation in Section 3 of the current induced by an external field in an unmatched transmission line is reduced to a time domain integration of the excitation with the (one dimensional) space – time Green's function as a kernel. This kernel can be represented as a sum of oscillator response functions multiplied by one dimensional spatial eigenmodes. It is shown that the amplitude of transient oscillations can be larger than the steady-state amplitude, if the line is excited by a switched – on sinusoidal pulse with frequency larger than the resonant frequency of the line. Moreover, by applying the SEM method [3] the results can be generalized for the high-frequency case, when the characteristic wavelength is less or comparable to the transverse dimension of the line and radiation has to be taken into account.

In Section 4 the same consideration is carried out for the excitation of the rectangular resonator by an electromagnetic wave penetrating through a small circular aperture. Again the solution in time domain is represented as a time – domain integral of the excitation with the (three – dimensional) space-time Green's function as a kernel. This kernel can be represented as a sum of products of spatial resonator eigenmodes and oscillator – like responses of each mode. It is shown that the expected effect also appears in this case.

The research of time-domain responses is important for investigations in a MSC that, of course, is a resonator with eigenfunctions that are different for different angles of the stirrer. However, in this case the pseudo – stochastic picture of the resonance excitation is observed. At the same time, the experiments in the MSC excited by pulse – modulated harmonic signals show that the considered effect can be observed for some frequencies of excitation and positions of the stirrer. In this case sensitive, fast digital circuits can fail although the averaged level of the pulse does not reach the threshold value. An experimental example is presented in Section 5. Concluding remarks and an outlook for further research conclude the paper with Section 6.

2 Oscillating Circuits

In many areas of physics the model of a harmonic oscillator is frequently used to describe (often phenomenologically) results of experiments. This occurs in everything from classical mechanics to electrodynamics and up to quantum mechanics. It concerns harmonic processes that often are related with resonance phenomena. In the investigations of this paper the harmonic oscillator will become a basic element. One of its simplest representations is an oscillating electrical circuit with one capacitance (C) and one inductance (L). Such a system is described by an ordinary differential equation (ODE) of second order

$$\ddot{q}(t)+\frac{R}{L}\dot{q}(t)+\frac{1}{LC}q(t)=u_s(t) \tag{1a}$$

or more general

$$\ddot{x}(t)+2\gamma\dot{x}(t)+\omega_0^2 x(t)=f(t) \tag{1b}$$

Here $x(t)$ denotes the oscillating quantity (e.g. charge), γ the damping coefficient, ω_0 the resonance frequency, and $f(t)$ the exciting force (e.g., voltage). The solution of (1b) is easily expressed with the aid of the Green's function

$$K(t)=\frac{1}{\widetilde{\omega}_0}\exp(-\gamma t)\sin(\widetilde{\omega}_0 t)h(t) \tag{2}$$

for this problem expressed as

$$x(t)=\int_{-\infty}^{t} f(t_1)\cdot K(t-t_1)dt_1 \tag{3}$$

The eigenfrequency $\widetilde{\omega}_0=\sqrt{\omega^2-\gamma^2}$ of the oscillator and the Heaviside function

$$h(t)=\begin{cases}1, & t>0\\ 0, & t<0\end{cases} \tag{4}$$

occur in the Green's function. Since it is assumed that the excitation is switched on at $t = 0$ the integration in (3) goes from 0 to t.
A simple example for an excitation function is a switched – on sine – function

$$f(t) = F\sin(\omega t)h(t) \tag{5}$$

Using this function in (1b) and performing the integration in (3) results in the general solution

$$x(t) = \frac{F}{\left(\omega^2 - \omega_0^2\right)^2 + 4\gamma^2\omega^2} \cdot \left\{ \underbrace{\left[2\gamma\omega\cos(\tilde{\omega}_0 t) + \frac{\omega}{\tilde{\omega}_0}\left(\omega^2 - \omega_0^2 + 2\gamma^2\right)\sin(\tilde{\omega}_0 t) \right]}_{\text{Transient part}} \exp(-\gamma t) + \right.$$

$$\left. + \underbrace{\left[(\omega^2 - \omega_0^2)\sin(\omega t) - 2\gamma\omega\cos(\omega t) \right]}_{\text{Steady-state part}} \right\} \cdot h(t) \tag{6}$$

which already shows all essential properties of a transient phenomenon. In this case it was possible to clearly separate analytically the transient part (early times) of the solution from the steady-state part (late times). Therefore, it suggests itself to investigate under which conditions the amplitude of the transient part of the solution $x(t)$ exceeds that of the steady-state part. Assuming that for early times ($\gamma t << 1$) the damping is much smaller than the excitation frequency ($\gamma << \omega_0$) and resonance frequency and excitation frequency are far apart from each other, then the general solution simplifies to

$$x(t) \approx \frac{F}{\omega_0^2 - \omega^2} \cdot \left[\underbrace{-\frac{\omega}{\omega_0}\sin(\omega_0 t)}_{\text{Transient part}} + \underbrace{\sin(\omega t)}_{\text{Steady-state part}} \right] \cdot h(t) \tag{7}$$

In this expression two cases are of interest:

- excitation frequency and resonance frequency are of the same order of magnitude or $\omega << \omega_0$

Then the steady state part dominates the transient one.

- "high frequency excitation": $\omega_0 << \omega$

Now the amplitude of the transient part exceeds that of the steady state part by approximately the factor of ω / ω_0.
In figures 1a and 1b a numerical example for the latter case is displayed with constants $\omega_0 = 1$, $\gamma = 0.1$, $\omega = 4$ and $F = 1$ (all values are given in arbitrary units).

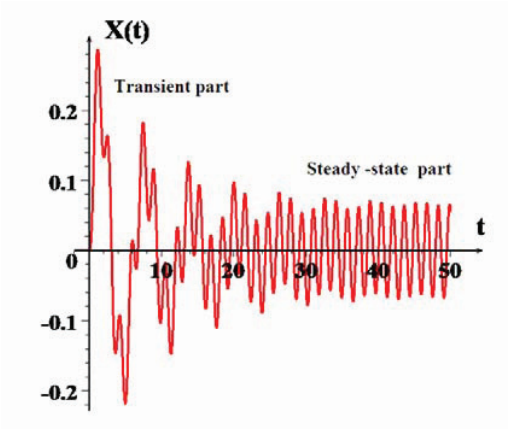

Fig. 1(a)

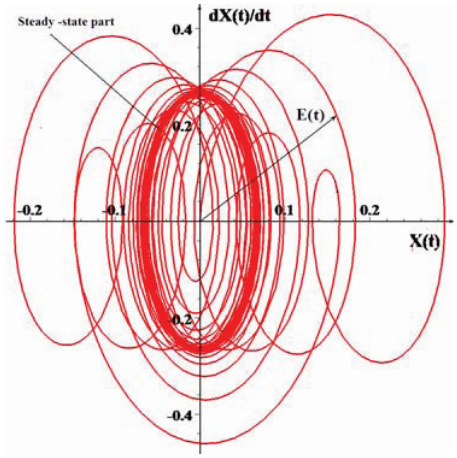

Fig. 1(b)

Figure 1: a). Amplitude $x(t)$ of the oscillations. b): Corresponding phase diagram $[x(t), \dot{x}(t)]$.

The amplitude of the transient part exceeds that of the steady state part by a factor of 3. This effect is also mirrored in the phase diagram by the typical "ear-effect".
Further excitation functions and corresponding response functions are assembled in Table 1 in the appendix.

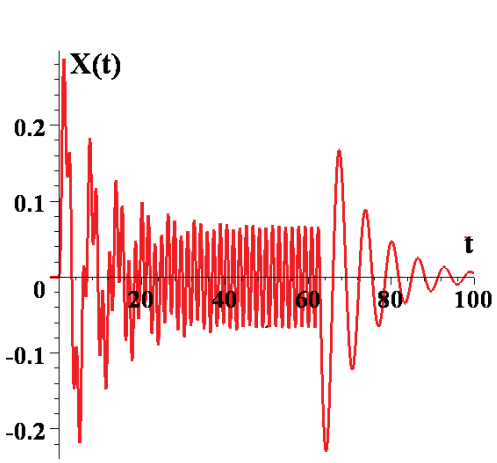

(a)

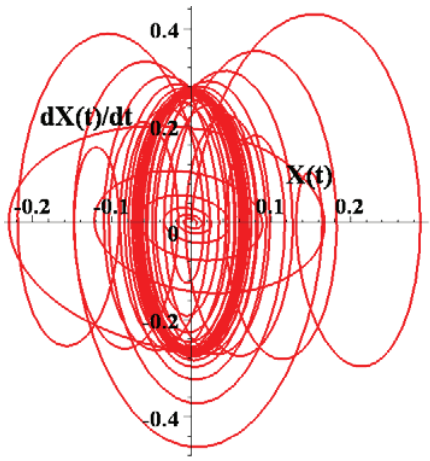

(b)

Figure 2: Response of a switched - on and - off sine excitation. a): Amplitude $x(t)$ b): Phase diagram $[x(t), \dot{x}(t)]$. $\omega_0 = 1$, $\gamma = 0.1$, $\omega = 4$, $N = 40$, $F = 1$ (arbitrary units)

It is interesting to note that for all these response functions (with the exception of the Gauss-pulse) the transient parts dominate the steady – parts (observe the "high – frequency" excitation parameters). Figures 2a and 2b exhibit the typical overshoots for a switched – on and switched - off process, an effect which plays an important role in EMC experiments with digital electronic devices.

3 Transmission Line as Resonator

In this section a simple classical lossless transmission line, parallely conducted above perfectly conducting ground, is analyzed. The line is terminated at both ends with the same resistance R and excited by a vertically incident plane wave. Length, height above ground, and radius of the line are denoted by the quantities L, h, and a, respectively.

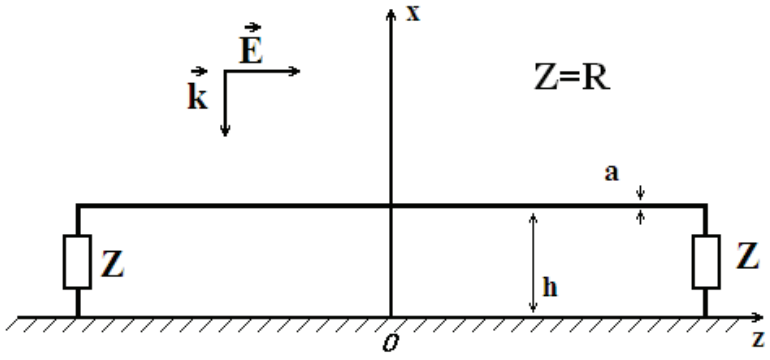

Figure 3: Excitation of a symmetrically terminated line by the vertical plane wave.

The induced scattered voltage $U(z)$ and induced current $I(z)$ along the line can be calculated with the aid of the well-known Telegrapher equation (in the Agrawal formulation) in frequency domain[1]

$$\begin{cases} \dfrac{dU}{dz} + j\omega L' I = E_z(j\omega, h) \\ \dfrac{dI}{dz} + j\omega C' U = 0 \end{cases} \tag{8}$$

and the symmetrical boundary conditions

$$\begin{aligned} U(-L/2) &= -Z \cdot I(-L/2) \\ U(L/2) &= Z \cdot I(L/2) \end{aligned} \tag{9}$$

The excitation function

$$E_z(j\omega, h) = E_0(j\omega) \cdot 2j \sin(kh) \tag{10}$$

does not depend on the local coordinate z. The inductance per unit-length L', the capacitance per unit-length C', and the characteristic impedance Z_C are given by

$$L' = \frac{\mu_0}{2\pi} \ln(2h/a); \qquad C' = \frac{2\pi\varepsilon_0}{\ln(2h/a)}; \qquad Z_C = \sqrt{L'/C'} \tag{11}$$

Due to the symmetrical terminations and the absence of a vertical component of the exciting E-field, one obtains the following solution from equations (8), (9)

$$I(z, j\omega) = \frac{E_z(j\omega, h)}{j\omega L'} \cdot \left[1 - \frac{Z}{Z + Z_C} \frac{e^{jk(L/2-z)} + e^{jk(L/2+z)}}{1 - \rho e^{-jkL}} \right] = E_z(j\omega, h) \cdot K(j\omega, z) \tag{12}$$

[1] It is noted that for a vertically incident electromagnetic wave a vertical component of the electric field is absent and the vertical part of the line does not act as a voltage source as is usual in the Agrawal formulation of the transmission line approximation.

with the Green's function $K(j\omega, z)$ in frequency domain and reflection coefficient ρ for the current waves

$$\rho = \frac{Z_C - Z}{Z_C + Z} \tag{13}$$

In order to find an analytical solution of (12) in time domain one separately transforms the Green's function and excitation function in time domain and subsequently performs the convolution

$$I(z,t) = \int_{-\infty}^{t} E_z(t', h) \cdot K(t - t', z) dt' \tag{14}$$

The causality condition requires

$$K(t, z) = 0 \qquad \text{for} \qquad t \le 0 .$$

The expansion of the denominator in (12) of the second term in the square bracket in a geometrical series

$$(1 - \rho \exp(-jkL))^{-1} = \sum_{n=0}^{\infty} \rho^n \exp(-jknL)$$

results in the following expression for the Green's function in time-domain

$$K(t,z) = \frac{1}{L'}\left\{ h(t) - \frac{Z}{Z + Z_C} \sum_{n=0}^{\infty} \rho^n \left[h(t - ((n+1/2)L - z)/c) + h(t - ((n+1/2)L + z)/c) \right] \right\} \tag{15}$$

The first term in the curly brackets reflects the response of an infinitely long line excited by a delta - like function. The terms behind the sum sign arise due to reflections at the ends of the line.

The convolution integral (14) has to be calculated for any fixed time t by using eq. (15). For each time this is achieved by a finite number of summands in (15). For early times the integral converges quite quickly if the excitation is a pure pulse. However, for periodical or quasi-periodical excitations a large number of summands has to be taken into account. To avoid long computation times it is recommended to calculate $K(j\omega, z)$ and apply the residue theorem.

From complex analysis it is known that one has to find the poles of the integrand in the complex plane. Assuming that the line has antenna-like terminations

$$R > Z_C \qquad \text{or} \qquad -1 < \rho < 0 \tag{16}$$

the poles can be found as

$$\omega_\infty = j\frac{R'}{L'}, \qquad R' \to 0 \tag{17}$$

(pole which appears for an infinitely long line)

$$\omega_n = \frac{c}{L}\left(2\pi(n+1/2) + j\ln(-1/\rho)\right), \qquad n = \ldots -2,-1,0,1,2\ldots \tag{18}$$

(poles which are correlated with the excitation of eigenmodes of a finite conductor).
With these poles and the use of the residue theorem one arrives at

$$\begin{aligned} K(z,t) = {} & \frac{1}{L'}\left[1 - 1/2\left[h(t - L/2c + z/c) + h(t - L/2c - z/c\right]\right] - \\ & - \frac{2Z}{Z + Z_C}\frac{c}{L}\sum_{n=0}^{\infty}\mathrm{Im}\left\{\frac{1}{\omega_n L'}\left[e^{j\omega_n(t - L/2c + z/c)}h(t - L/2c + z/c) + \right.\right. \\ & \left.\left. e^{j\omega_n(t - L/2c - z/c)}h(t - L/2c - z/c)\right]\right\} \end{aligned} \tag{19}$$

For times $t > \max\left[(L/2+z)/c, (L/2-z)/c\right]$ the Green's function can be expressed as a sum of modal Green's functions $K_n(t,z)$

$$K(t,z) = -\frac{2Z}{Z + Z_C}\frac{c}{L}\sum_{n=0}^{\infty}\mathrm{Im}\left[\frac{\exp(j\omega_n(t - L/2c))\cdot\cos(\omega_n z/c)}{\omega_n L'}\right] = \sum_{n=0}^{\infty}K_n(t,z) \tag{20}$$

Each individual Green's function $K_n(t,z)$ resembles that of equation (2) with the difference that now an infinitely number of eigenfunctions occur and the modal Green's functions are consecutively numbered. This similarity becomes even more visible in the case of the line with open ends. Then the imaginary parts of the eigenfrequencies vanish and (20) yields

$$K_n(t,z) = -\frac{4Z}{Z + Z_C}\frac{c}{L}\frac{\sin(\omega_n(t - L/c))\cdot\cos(\omega_n z/c)}{\omega_n L'} \tag{21}$$

Thus the line is represented as a set of oscillators which are driven by an exterior force (electrical field). The amplitudes of individual oscillators decrease with increasing n, if the exciting frequencies do not coincide with any eigenfrequency of the oscillators. Otherwise they can become even larger.
In the following, two numerical examples are chosen to demonstrate dominating transient parts of the response functions.
First, a transmission line of 10 m length and radius of 1 cm is conducted 50 cm above perfectly conducting ground. It is terminated at both ends with 2000 Ω and excited by a double – exponential plane wave

$$E_0(t) = E_0 \cdot Q \cdot (e^{-\alpha t} - e^{-\beta t})h(t) \tag{22}$$

with the parameters $E_0 = 1$ V/m, $Q = 1.05$, $\alpha = 1\cdot 10^7$ s^{-1} and $\beta = 1\cdot 10^8$ s^{-1}.
The time-domain behavior of the current in the middle of the line is shown in Figure 4.

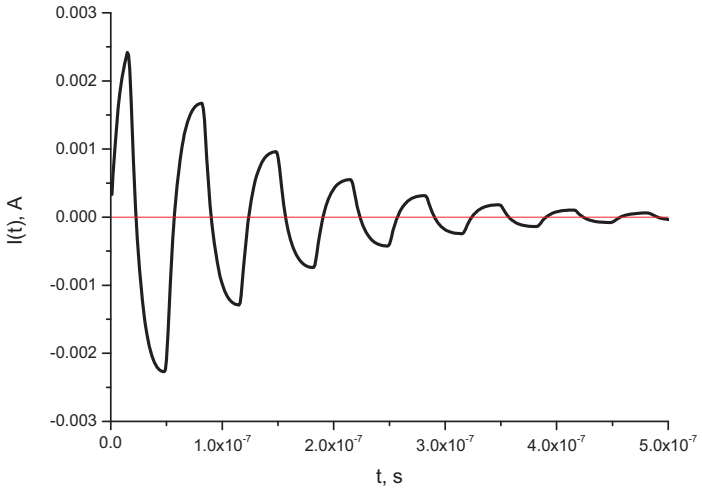

Figure 4: Transmission line response for a double exponential excitation.

One recognizes a relatively long lasting pulse – response compared to the decay time of the excitation function, which approximately corresponds to the delay time along the line. The current amplitude almost oscillates at its lowest frequency f_0=15 MHz.
In the second example the time-domain part of the excitation function is changed. The excitation is carried out by a switched – on, damped sine function

$$E_0(t) = E_0 e^{-\alpha t} \sin(2\pi f t) h(t) \tag{23}$$

with the quantities $E_0 = 1$ V/m, $\alpha = 1 \cdot 10^6$ s^{-1}, and $f = 67$ MHz. This excitation frequency is larger than the lowest resonance frequency (15 MHz) and is different from the subsequent lower eigenfrequencies $f_1 = 45$ MHz, $f_2 = 75$ MHz, and $f_3 = 105$ MHz.
In Fig. 5 the current in the middle of the line is displayed again.

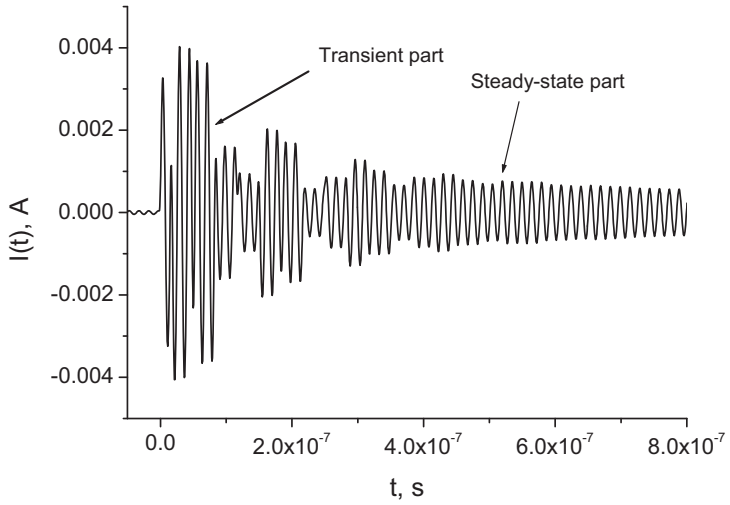

Figure 5: Line response for a damped sine excitation.

As in the previous section, a dominant transient part can be observed. Even beat effects with a frequency of about 8 MHz (difference between f_2 and the excitation frequency) can be seen.

Note that the investigated case of a transmission line is not the most general one. However, even arbitrary directions of incidence for the plane wave and arbitrary terminations would not change the principal results. Moreover, for high frequencies one could include radiation phenomena. Then one would use the "Singular Expansion Method" [3]. The Green's function in frequency domain then can be written as a sum whose summands have the form of the inverse Fourier transformation of eq. (2). The radiation losses are contained in the imaginary parts of the resonance frequencies (compare with eq. (20)).

4 Rectangular 3-dimensional Resonator

In this section a rectangular cavity is examined that is excited through a circular aperture by an exterior plane wave (see Figure 6). It will be demonstrated that for this system the same effects as in the previous configurations also arise here: With appropriate parameter choice the transient portion of the field in the cavity clearly predominates that of the steady – state.

The following representation is divided into subsequent steps: in the first step the coupling of an incoming plane wave through a small aperture of the thin cavity screen is described. The aperture is treated as a combination of an electrical and magnetic dipole. After that, different representations of the Green's function in frequency – and time - domain follow. Eventually, the transient and steady – state parts of the fields are calculated, and a brief explanation of how the time-domain results can be used to deal with linear and non-linear scatteres within a resonator is given.

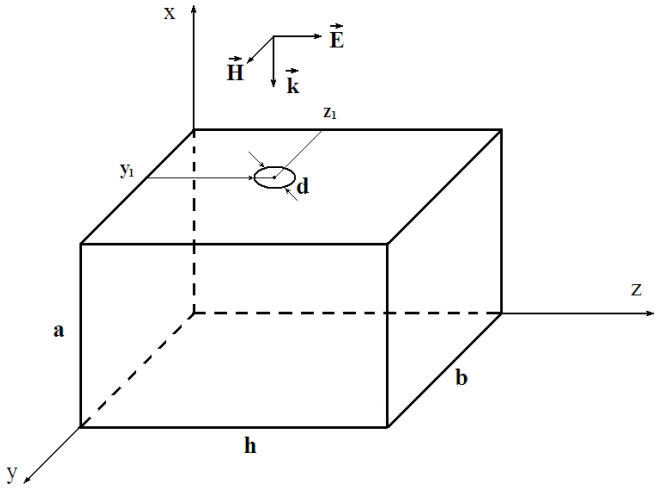

Figure 6: Excitation of a 3-dim. resonator through a circular aperture.

To calculate the interior field that is coupled through the small aperture ($kd << 1$, d diameter of the hole), the electric ($\vec{P}$) and magnetic ($\vec{M}$) dipole-moments in the aperture plane are needed. These moments are obtained with the aid of the scattered normal electric field $\vec{E}_{\perp,sc}$ and the tangential magnetic field $\vec{H}_{\parallel,sc}$ as [4, p.188]

$$\vec{P}_{\perp} = \alpha_e \varepsilon_0 \vec{E}_{\perp,sc}\,; \qquad \vec{M}_{\parallel} = -\hat{\alpha}_m \vec{H}_{\parallel,sc}\,, \tag{24 a,b}$$

For the considered simple aperture the components of the polarisability tensor are known [4, p.441]:

$$\alpha_e = \frac{1}{12} d^3 \qquad \alpha_{m,x} = \alpha_{m,y} = \frac{1}{6} d^3 \tag{25 a,b}$$

To obtain the fields in (24) the associated scattering problem has to be solved. With the conditions $\lambda >> b, h$ [2] one arrives at

$$E_{sc,\perp} = E_{sc,x} = 0\,, \qquad H_{sc,y} = 2H_0 = 2E_0/\eta_0\,, \qquad H_{sc,z} = 0\,. \tag{26}$$

Here E_0 and H_0 are the amplitudes of the incoming field. With these values the dipole moments yields

$$\vec{P} = \vec{0} \qquad M_x = M_z = 0 \qquad M_y = -\frac{d^3}{3} H_0 \tag{27}$$

Next, the connection to the corresponding magnetic current sources is required:

$$d\vec{J}^{\,M} = \int_{\substack{\text{region of} \\ \text{source}}} \vec{j}^{\,M}(\vec{r}\,')dV' = j\omega\vec{M}(j\omega) \tag{28}$$

Thus, the current sources in the resonator are known and from them the electric field can be derived as soon as one knows the magnetic vector potential $\vec{A}_M$ [6] from the magnetic currents [5, 6]:

$$\vec{E}(\vec{r}) = -curl_{\vec{r}}\,(\vec{A}^{\,M}(\vec{r})) \tag{29}$$

At this point, in order to prevent a comprehensive and difficult derivation of the electrical field from the above equations only the final result in frequency domain is given that is dependent on the magnetic moment[3]. Due to the special excitation (E-field parallel to the surface) the electric dipole does not contribute to the electric field inside the resonator.

$$\vec{E}(j\omega,\vec{r}) = \frac{\mu_0}{4\pi} \sum_{v} \frac{j\omega}{r_v^2} \left\{ \frac{1}{r_v^2} + jk \right\} \left[\vec{r}_v, \hat{T}_v^{M} \cdot \vec{M}(j\omega) \right] \exp(-jkr_v) \tag{30}$$

Here, the indices n_1, n_2, n_3 denote the number of reflections at the walls in x, y,z – direction. The summation is carried out for all "index –vectors" $|v\rangle := |n_1, n_2, n_3\rangle$ from $-\infty$ to ∞. The quantity $\vec{r}_v = \vec{r} - \vec{R}_v$ indicates the distance between the radius vector of the observation point $\vec{r}$ and the radius – vector $\vec{R}_v$ for the position of the v^{th} reflection image:

---

[2] For simplification of the external problem an infinite perfectly conducting screen (i.e. the top of the parallelepiped in Fig. 6 is continued to infinity) is considered.

[3] A simple generalization of the ray approximation in time domain for a rectangular resonator is used [8].

$$\vec{R}_v = (X(n_1), Y(n_2), Z(n_3))$$
$$X(n_1) = x_1 \cdot (-1)^{n_1} + \left((1-(-1)^{n_1})/2 + n_1\right) \cdot a\,,$$
$$Y(n_2) = y_1 \cdot (-1)^{n_2} + \left((1-(-1)^{n_2})/2 + n_2\right) \cdot b\,,$$
$$Z(n_3) = z_1 \cdot (-1)^{n_3} + \left((1-(-1)^{n_3})/2 + n_3\right) \cdot h \qquad \text{(31 a, b, c, d)}$$

The quantity $\hat{T}_v^M$ is the transformation matrix for multiple reflections of the magnetic moment:

$$\hat{T}_v^M = \begin{pmatrix} (-1)^{n_1} & 0 & 0 \\ 0 & (-1)^{n_2} & 0 \\ 0 & 0 & (-1)^{n_3} \end{pmatrix} \qquad (32)$$

The inverse Fourier transformation of (30) yields the time-domain result for the electric field inside the resonator

$$\vec{E}(t,\vec{r}) = \frac{\mu_0}{4\pi} \sum_v \left\{ \frac{1}{r_v^3} \left[\vec{r}_v, \hat{T}_v^M \cdot \dot{\vec{M}}(t_v) \right] + \frac{1}{c r_v^2} \left[\vec{r}_v, \hat{T}_v^M \cdot \ddot{\vec{M}}(t_v) \right] \right\} \qquad (33)$$

with the retarded time $t_v = t - r_v / c$ of the v^{th} mirror image.

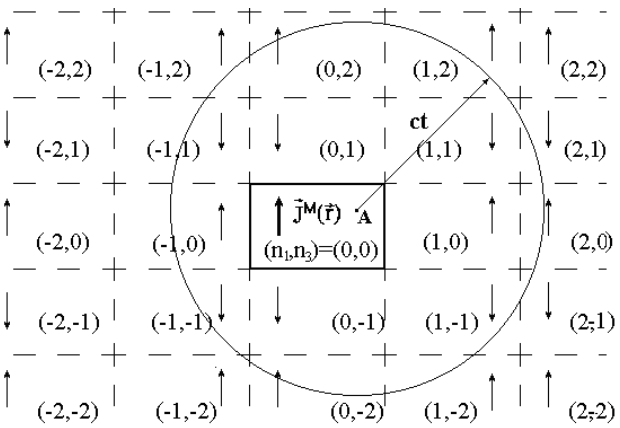

Figure 7: Reflection scheme for a 2-dim. rectangular structure.

Assuming the magnetic moment $\vec{M}(t)$ $(t \geq 0)$ in (33) is known for all t then the sum (33) can be approximated by a finite number of summands which are defined for $t_v \geq 0$. In other words: the number of non-vanishing summands can be restricted by a natural number N_Σ which is obtained by means of a sphere with radius ct (see Figure 7):

$$N_\Sigma(t) \approx Int\left(4\pi/3 \cdot (ct)^3 / V\right) \qquad (34)$$

(V volume of the resonator)

Therefore, a computer calculation for the three – fold sum (33) is quickly performed. It should be emphasized that the summation of mirror – images and its restriction to a sphere of radius $\sim ct/\sqrt[3]{V}$ only affects the transient part of the response function. For later times one has to add many more terms in (33). In this case eq. (30) should be transformed into an eigenmode representation. Then the electrical field reads as follows in the frequency domain:

$$E_x(j\omega,\vec{r}) = -\frac{4}{3}\frac{d^3}{V}\sum_{\substack{n_x=0\\ n_y=1\\ n_z=1}}^{\infty}(2-\delta_{0,nx})\cos(k_x x)\cos(k_x x_1)\sin(k_y y)\sin(k_y y_1)\cdot$$

$$\cdot\sin(k_z z)\cos(k_z z_1)\cdot k_z\cdot\underbrace{\frac{jkE_0(j\omega)}{k_v^2-k^2+j\delta}}_{F_v(j\omega)} \tag{35}$$

$$E_y(j\omega,z) = 0 \tag{36}$$

$$E_z(j\omega,\vec{r}) = \frac{4}{3}\frac{d^3}{V}\sum_{\substack{n_x=1\\ n_y=1\\ n_z=0}}^{\infty}(2-\delta_{0,nz})\cdot k_x\sin(k_x x)\cos(k_x x_1)\sin(k_y y)\sin(k_y y_1)\cdot$$

$$\cdot\cos(k_z z)\cos(k_z z_1)\cdot\underbrace{\frac{jkE_0(j\omega)}{k_v^2-k^2+j\delta}}_{F_v(j\omega)} \tag{37}$$

Here the eigenmode numbers $|v\rangle := |n_x,n_y,n_z\rangle$ are connected to the eigenvector wave values as

$$|k_x,k_y,k_z\rangle := |\pi n_x/a,\pi n_y/b,\pi n_z/h\rangle \tag{38}$$

and as $k_v = \sqrt{(\pi n_x/a)^2+(\pi n_y/b)^2+(\pi n_z/h)^2}$ with $\omega_v = k_v/c$.

At this point it is appropriate to introduce the function

$$F_v(j\omega) = \frac{jkE_0(j\omega)}{k_v^2-k^2+j\delta} \qquad \delta\to 0 \tag{39}$$

The parameter δ characterizes the resonator losses in the walls. These losses can be included by changing the wave number

$$k\to k\cdot\left(1-\frac{j}{2Q(k)}sign(k)\right) \tag{40}$$

where $Q(k)$ denotes the quality factor of the resonator (caused, for example, by the losses in the walls), and the quantity $sign(k)$ is introduced to conserve causality. If it is assumed that in the neighborhood of the v^{th} resonance the Q - factor can be approximated by

$$Q(k) \approx Q(k_v),$$

then one can re-write (39) as

$$F_v(j\omega) = \frac{jc\omega E_0(j\omega)}{\omega_v^2 + \gamma_v^2 + 2j\omega\gamma_v - \omega^2}, \qquad \gamma_v = k_v / 2Q(k_v) \tag{41}$$

After performing the Fourier transformation of eqs. (35)- (37) using eq. (41) one of the key results is obtained, namely the electrical field components in time domain:

$$E_x(t,\vec{r}) = -\frac{4}{3}\frac{d^3}{V}\sum_{\substack{n_x=0\\n_y=1\\n_z=1}}^{\infty}(2-\delta_{0,n_x})\cos(k_x x)\cos(k_x x_1)\sin(k_y y)\sin(k_y y_1)\sin(k_z z)\cos(k_z z_1)k_z F_v(t) \tag{42}$$

$$E_y(t,z) = 0 \tag{43}$$

$$E_z(t,\vec{r}) = \frac{4}{3}\frac{d^3}{V}\sum_{\substack{n_x=1\\n_y=1\\n_z=0}}^{\infty}(2-\delta_{0,nz})\sin(k_x x)\cos(k_x x_1)\sin(k_y y)\sin(k_y y_1)\cos(k_z z)\cos(k_z z_1)k_x F_v(t) \tag{44}$$

with $$F_v(t) = c\int_{-\infty}^{t}\frac{\partial}{\partial t_1}E_0(t_1)\cdot\underbrace{e^{-\gamma_v(t-t_1)}\frac{\sin\omega_v(t-t_1)}{\omega_v}}_{K_v(t-t_1)}dt_1 \tag{45}$$

and $$K_v(t) = e^{-\gamma_v t}\frac{\sin\omega_v t}{\omega_v}h(t) \tag{46}$$

Equations (45) and (46) are quite revealing; they coincide with equations (2) and (3) if one chooses $\omega_0 \to \sqrt{\omega_v^2 + \gamma_v^2}$, $\gamma \to \gamma_v$, $\tilde{\omega}_0 \to \omega_v$. Thus it is possible to reduce – as in the case of the transmission line – the excitation of a 3-dim. resonator in time domain to the excitation of infinitely many oscillators. The driving force of any oscillator contains the parameters of the aperture, position dependent eigenfunctions of the resonator, and the time derivative of the exterior field. Therefore, the following also holds true for the excitation of the chamber: In case of a high frequency excitation the amplitude of the transient part of the field exceeds that of the steady-state part. Next, a numerical example is investigated. The resonator has the dimensions a =1 m, b=2 m, h=3 m, and a circular aperture with diameter d=0.05m at the position x1=a, y1=0.1m, z1=0.3m. It is excited by a switched-on sine function with parameters E_0=1 V/m, f_0=10 GHz. The excitation frequency is much larger than the smallest eigenfrequency of the resonator $f_{v0} = 90.14$ MHz.

$$E_0(t) = E_0\sin(\omega_0 t)h(t) \tag{47}$$

With this function the response function (eq. 45) becomes

$$F_v(t) = \frac{E_0 \omega_0}{2k_v} \mathrm{Im}\left\{ \frac{e^{j\omega_0 t} - e^{j\omega_v t - \gamma_v t}}{\gamma_v + j(\omega_0 - \omega_v)} - \frac{e^{j\omega_0 t} - e^{-j\omega_v t - \gamma_v t}}{\gamma_v + j(\omega_0 + \omega_v)} \right\} \tag{48}$$

The field component $E_x(t)$ and $E_z(t)$ were calculated numerically. The results are shown in Figures 8 and 9. Again, non-surprising effects can be observed: The transient amplitude of the

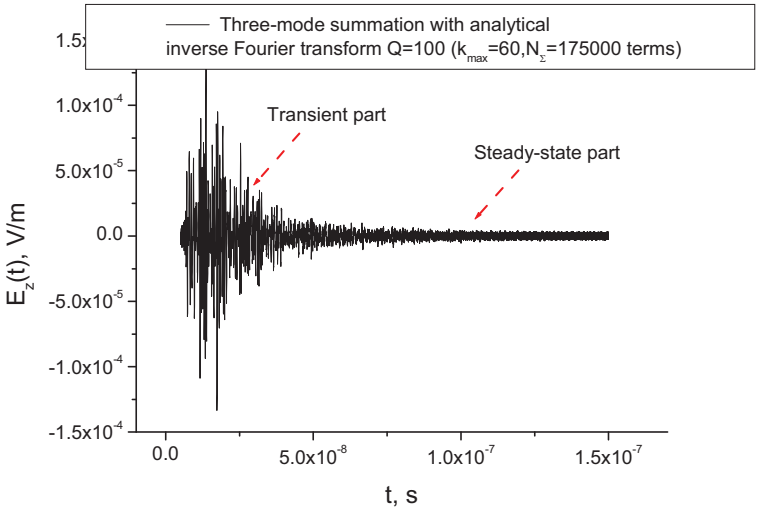

Figure 8: Electrical field component $E_x(t)$ inside the cavity.

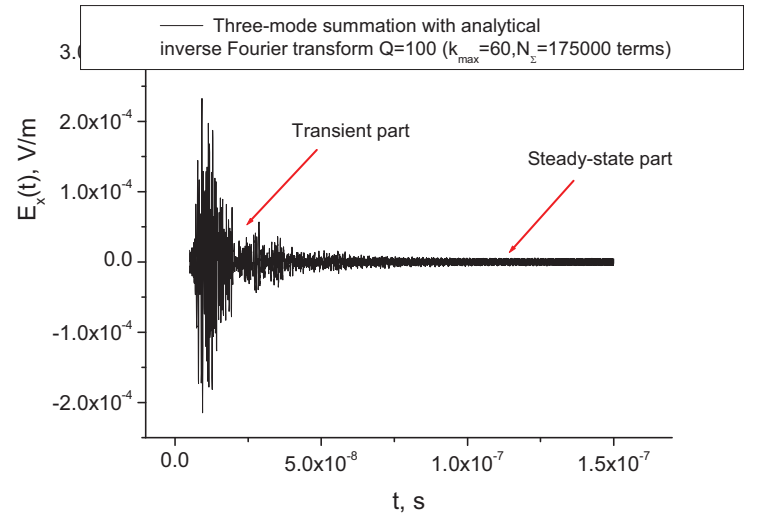

Figure 9: Electrical field component $E_z(t)$ inside the cavity.

field prevail and beat effects are clearly seen due to the close neighborhood of eigenfrequencies. The above results provide the basis for further investigations. Of particular interest are the interactions of shielded enclosures (resonators) with modern digital non-linear electronics.

5 Experiments

This section serves as experimental evidence of the effect of the transient part of a pulse response. First, the empty MSC is examined with a switched – on and switched – off sinusoidal function. The stirrer positions are different but are fixed during the experiment. Second, the threshold values of a modern digital processor are determined. The excitations are carried out with pulses of different pulse widths, with different repetition rates, and with different frequencies.

5.1 Field distributions in mode stirred chambers

Pulse excitations of an MSC were carried out at both the Fraunhofer Institute (INT) in Euskirchen and at the Otto-von-Guericke University in Magdeburg [7], in the respective usable frequency regions of the chambers. At this point, two selected curves that are representative for the performed measurements are displayed in Figures 10 and 11 for the envelope and the average over all envelopes of the electric field in the working volume of the INT mode stirred chamber. The sharp jagged curves in the figures represent the envelopes of the electric field strength at stirrer positions of 90° and 230°, respectively. The slightly smoother curves show the electric field distributions which arise after averaging over all stirrer positions. The predicted phenomena are visible: the overshoots are clearly pronounced and beat phenomena can be seen in the transient portion of the field strengths. It can also be seen that the plateaus of the steady-state parts of the fields at fixed stirrer positions can have different relative amplitudes compared to the plateau values of the averaged fields. Thus, if one would take the averaged curves as a basis for EMC tests then – as opposed to reality – no interference with the transient parts is to be expected.

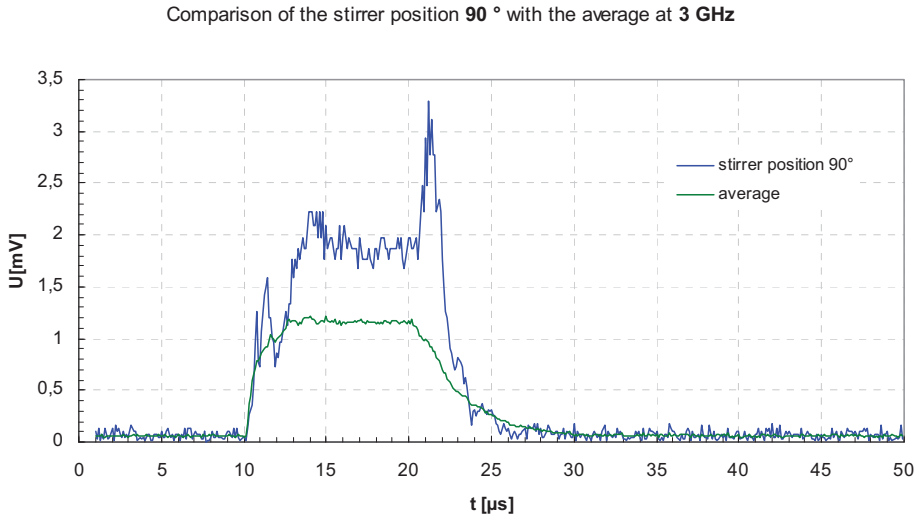

Figure 10: Envelopes of time - responses of the electrical field in an MSC for the stirrer position of 90° and averaged over all stirrer positions.

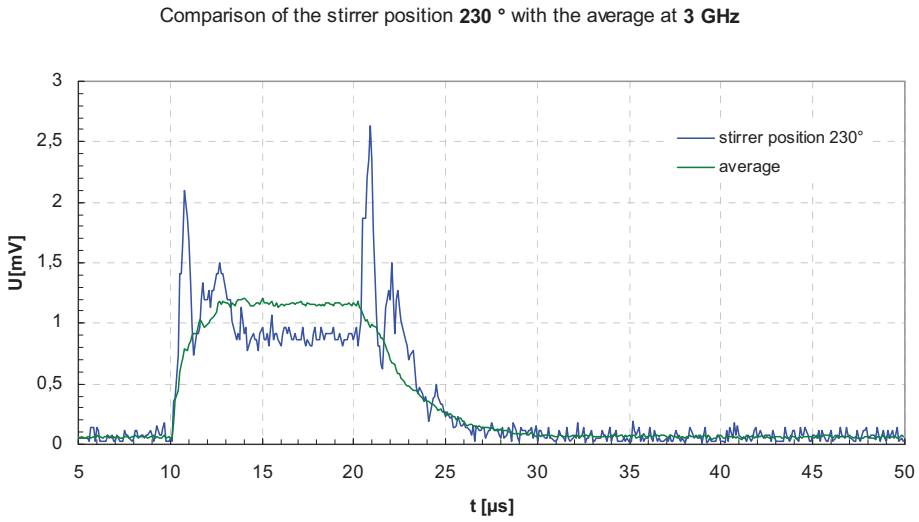

Figure 11: Envelopes of time - responses of the electrical field in an MSC. Stirrer position 230° and averaged over all stirrer positions.

5.2 Effects of the transient excitation part on modern electronics

To show the experimental evidence of the transient excitation the following experiment was conducted in the TEM – waveguide of the INT: A modern, digital processor, powered by a battery, was irradiated and its function was checked via optical fibers. Figure 12 shows the experimental setup. Excitation pulses were used with different pulse widths, repetition rates, and frequencies. Distortion thresholds were measured. The curves in Figure 13 display the thresholds. The chosen pulse widths and repetition rates are 200 ns and 1 µs, and 1 Hz and 1000 Hz, respectively.

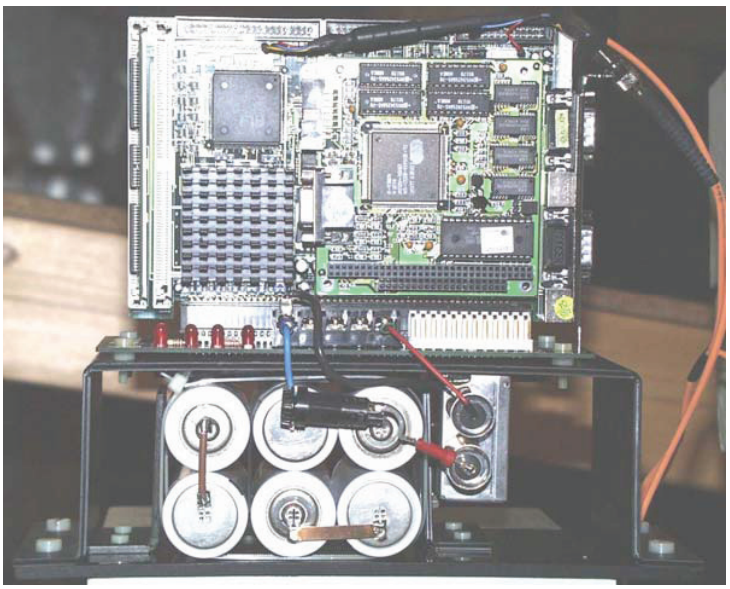

Figure 12: Test setup of a modern processor in a TEM wave guide.

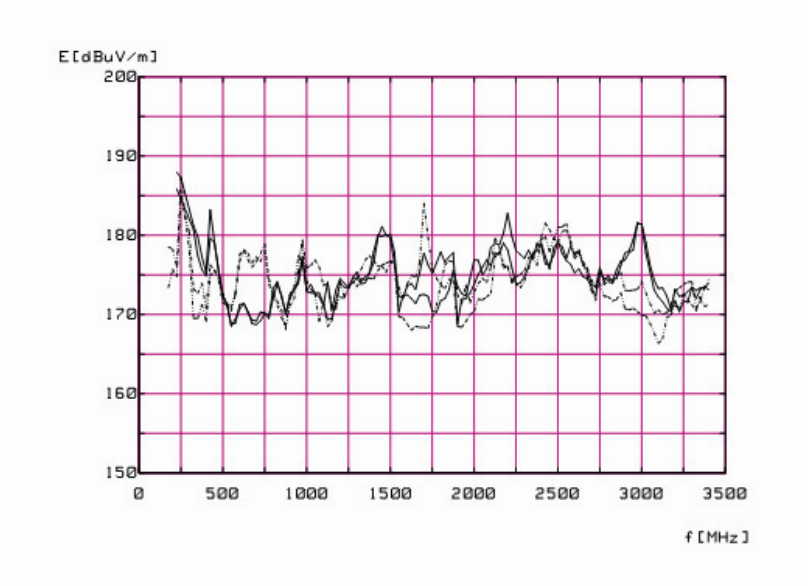

Figure 13: Influence of pulsed microwave signals on a digital high – speed computer (175dBμV/m = 562 V/m). Solid lines: E – field perpendicular to the circuit board; dashed lines: E – field parallel to the board.

The result is very interesting. The high frequency limit of the transistors in the circuit boards is virtually independent of the threshold pulse width, pulse repetition rate and radiation frequency. Compared to previous experiments, these measurements show a significantly different behavior. In analog circuits, the signals leading to failure are produced by rectification (demodulation) of the pulsed HF – signal. Since here the relevant circuit parts as well as the semiconductors have lowpass behavior, the interference threshold depends on the pulse width and repetition rate. This is not the case for high-speed digital technology. Instead it appears that in today's fast microprocessors the binary states are already influenced by the first half-wave of the HF – sine pulse, and thus by the early transient part of the exciting pulse.

6 Conclusion

In this paper analytical time-domain solutions for resonating systems (circuit, TL, cavity) were presented and discussed. It turned out that for all of these systems the time-dependent part of the corresponding modal Green's functions have the same structure and thus fulfill the same second order ODE. Therefore, it is not surprising that all response functions for pulse excitations exhibit the same principal behavior: namely, they contain transient and steady-state parts. For certain parameter choices for the excitation, the transient response amplitudes exceed those of the steady – state. It was shown that this may have an effect on modern digital electronics. EMC testing procedures (standards) that only place restrictions on CW – excitations can therefore overlook weaknesses of the system. Time – domain test methods are preferable in such cases. Since all our results were obtained in time-domain and could also be represented as sums over eigenmode functions that fulfil oscillating linear ODEs at any local point of the considered resonator, it is evident that future investigations can easily extend these equations and apply them to non-linear circuit elements and/or scatterers (an example is given in [9]). This, together with more experiments which confirm the discussed behaviour of modern digital electronics will become a future research subject.

References

1. H. U. Schmidt, Fraunhofer Institute (INT), Euskirchen, Germany, private communication.
2. Gantmacher, F.R.: The Theory of Matrices, Volume 2, Chelsea Publishing Company, New York, USA, 1984.
3. F.M.Tesche, M. V. Ianoz, T. Karlsson, EMC Analysis Methods and Computational Models, Willey&Sons, 1997.
4. K.S.H. Lee (editor): *EMP Interaction: Principles, Techniques, and Reference Data,* Taylor and Francis, Washington, DC, 1995, ISBN 1-56032-455-4
5.G.T. Markov, A.F. Chaplin, Excitation of Electromagnetic Waves, Moscow, "Radio I Svjaz' ", 1983 (Rus.) ("Vozbujshdenie Elektromagnitnuh Voln").
6. G. S. Smith, An introduction to classical electromagnetic radiation, Cambridge University Press, 1997.
7. J. Nitsch et. al. (OvGU), S. Potthast (WIS), Ch. Adami et. al. (INT), EME Symposium, Mannheim, 14. – 16.09. 2009, CD
8. S.V.Tkatchenko, G.V.Vodopianov, L.M. Martynov, "On the theory of the short - rise pulse penetration into rectangular cavities," 11th International Zurich Symposium and Technical Exhibition on Electromagnetic Compatibility, March 7 - 9, 1995, pp.513 - 518.
9. H.G. Krauthäuser, S.V. Tkachenko, J. Nitsch, "Strong Linear and Non-Linear Coupling to System-Cavity Modes from Repetitive High Frequency Illumination", Proceedings of the International Conference on Electromagnetics in Advanced Applications (ICEAA 01), 10-14 September, 2001, ISBN 88-8202-098-3.

Appendix

Table 1: Response functions of oscillating systems for different excitations

Excitation	Exciting function $f(t)$	Response function $x(t)$	Relation between parameters to observe the effect
"switched-on" sine function	$F\sin(\omega t)h(t)$	$x(t)=\frac{F}{\left(\omega^2-\omega_0^2\right)^2+4\gamma^2\omega^2}\cdot\left\{\left[2\gamma\omega\cos(\tilde{\omega}_0 t)+\frac{\omega}{\tilde{\omega}_0}\left(\omega^2-\omega_0^2+2\gamma^2\right)\sin(\tilde{\omega}_0 t)\right]\exp(-\gamma t)+\right.$ $\left.+\left[(\omega^2-\omega_0^2)\sin(\omega t)-2\gamma\omega\cos(\omega t)\right]\right\}\cdot h(t)$	$\omega >> \omega_0$
"switched-off" sine function	$F\sin(\omega t)h(-t)$	$x(t)=\frac{F}{\left(\omega^2-\omega_0^2\right)^2+4\gamma^2\omega^2}\cdot\begin{cases}-2\gamma\omega\cos(\omega t)+\left(\omega_0^2-\omega^2\right)\sin(\omega t), & t\le 0\\ \left[-2\gamma\omega\cos(\tilde{\omega}_0 t)+\frac{\omega}{\tilde{\omega}_0}\left(\omega_0^2-\omega^2-2\gamma^2\right)\sin(\tilde{\omega}_0 t)\right]\exp(-\gamma t), & t\ge 0\end{cases}$	$\omega >> \omega_0$
Finite sine function "switched-on" and "switched-off"	$F\sin(\omega t)\cdot$ $(h(t)-h(t-NT))$ $T:=2\pi/\omega,$ $N=1,2,3\ldots$	$x(t)=\frac{F}{2\tilde{\omega}_0}\begin{cases}\mathrm{Im}\left[\frac{\exp(j\Omega t)-\exp(j\omega t)}{\omega-\Omega}+\frac{\exp(j\Omega t)-\exp(-j\omega t)}{\omega+\Omega}\right]h(t), & t\le NT\\ \mathrm{Im}\left[\frac{2\omega\exp(j\Omega t)\left(1-\exp(-j\Omega N t)\right)}{\omega^2-\omega_0^2+2\gamma^2-2j\tilde{\omega}_0\gamma}\right], & t\ge NT\end{cases}$, $\Omega:=\tilde{\omega}_0+j\gamma$	$\gamma T\ge 1$ $\omega >> \omega_0$

Table 1: (Cont.) Response functions of oscillating systems for different excitations

Excitation	Exciting function $f(t)$	Response function $x(t)$	Relation between parameters to observe the effect
Sine function modulated by double exponential function	$F\sin(\omega t)\cdot$ $(e^{-\alpha t}-e^{-\beta t})h(t)$	$x(t)=F\omega\,\mathrm{Im}\left\{\frac{1}{\omega-\tilde{\omega}_0+j(\beta-\gamma)}\cdot\left[\frac{1}{\omega}\cdot\frac{\exp(j\omega t-\beta t)}{\omega+\tilde{\omega}_0+j(\beta-\gamma)}-\frac{1}{\tilde{\omega}_0}\cdot\frac{\exp(j\tilde{\omega}_0 t-\gamma t)}{\omega+\tilde{\omega}_0-j(\beta-\gamma)}\right]-\right.$ $\left.-\frac{1}{\omega-\tilde{\omega}_0+j(\alpha-\gamma)}\cdot\left[\frac{1}{\omega}\cdot\frac{\exp(j\omega t-\alpha t)}{\omega+\tilde{\omega}_0+j(\alpha-\gamma)}-\frac{1}{\tilde{\omega}_0}\cdot\frac{\exp(j\tilde{\omega}_0 t-\gamma t)}{\omega+\tilde{\omega}_0-j(\alpha-\gamma)}\right]\right\}\cdot h(t)$	$\omega >> \omega_0$ $\alpha << \gamma$ $\beta >> \gamma,\alpha$
Sine function modulated by a Gauss pulse	$F\sin(\omega t)\cdot e^{-(\alpha t)^2}$ $-\infty < t < \infty$	$x(t)=\frac{F\exp(-\gamma t)\sqrt{\pi}}{4\tilde{\omega}_0\alpha}\,\mathrm{Im}\left\{\exp\left[j\tilde{\omega}_0 t+\frac{(\gamma+j(\omega-\tilde{\omega}_0))^2}{4\alpha^2}\right]\cdot\left[1+erf\left(\alpha t-\frac{(\gamma+j(\omega-\tilde{\omega}_0))}{2\alpha}\right)\right]-\right.$ $\left.-\exp\left[-j\tilde{\omega}_0 t+\frac{(\gamma+j(\omega+\tilde{\omega}_0))^2}{4\alpha^2}\right]\cdot\left[1+erf\left(\alpha t-\frac{(\gamma+j(\omega+\tilde{\omega}_0))}{2\alpha}\right)\right]\right\}$ $erf(z)=\frac{2}{\sqrt{\pi}}\int_0^z\exp(-z_1^2)dz_1$ - integral exponent	